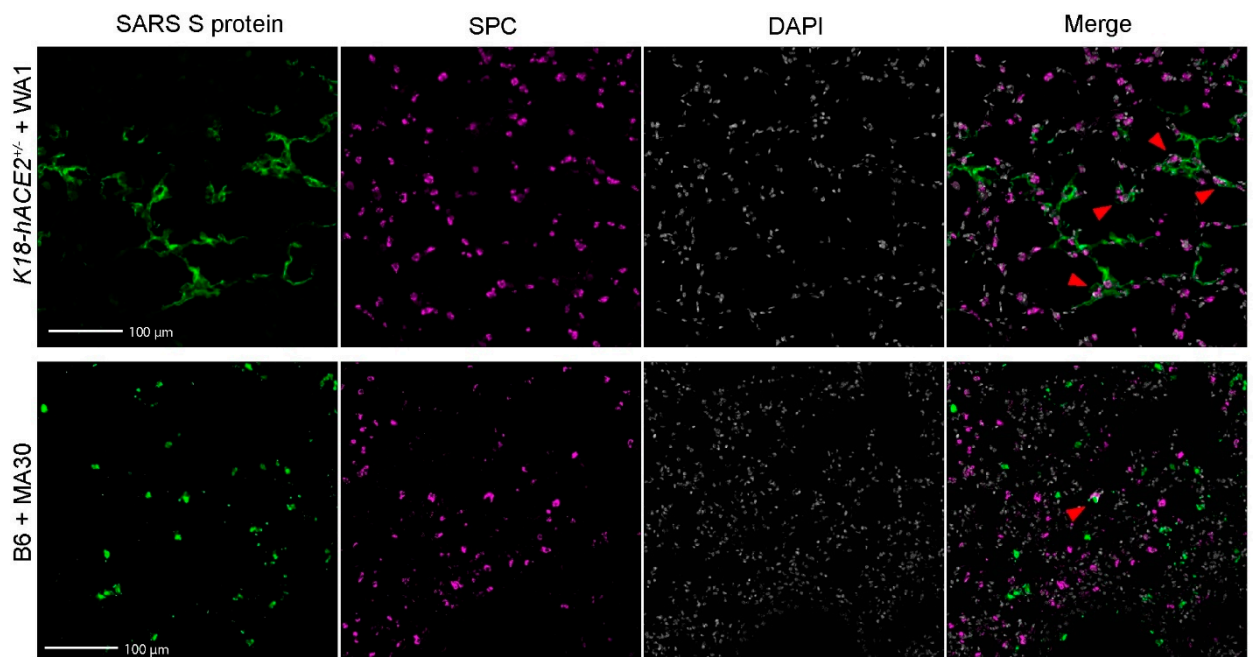
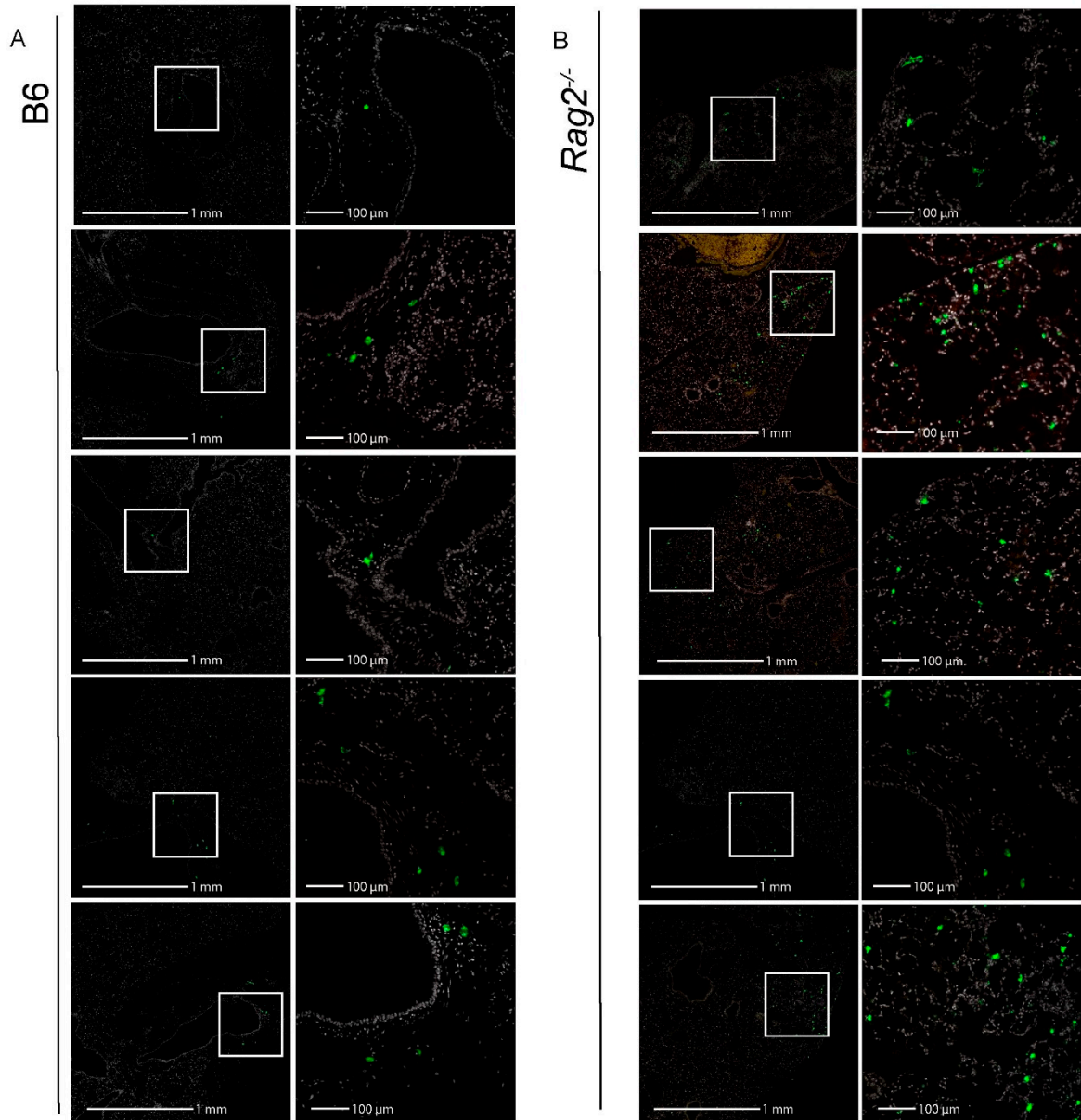


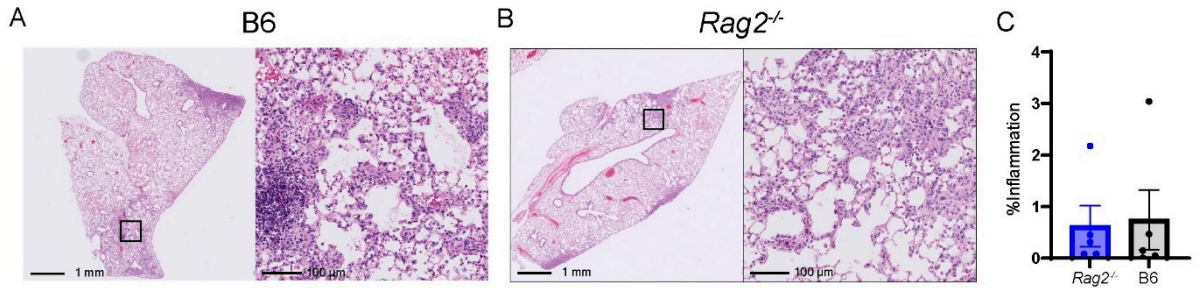
Supplemental Figure S1 SARS-CoV-2 infecting cell types and damage of the bronchial wall in the MA30-infected B6 and WA1-infected *K18-hACE2* mice. (A) Representative image of infection of alveolar cells (pointed by red arrows) by MA30 in B6 murine lungs at 3 DPI (A) and infection of peribronchial cells (pointed by red arrow) by WA1 in *K18-hACE2^{+/+}* murine lungs at 3 DPI. (C) Images of serial sections showing sloughing of infected and necrotic epithelial cells within the bronchus in H/E (left panel, red arrow) and in immunofluorescence (right panel, red arrow) with anti-SARS in green and DAPI white.



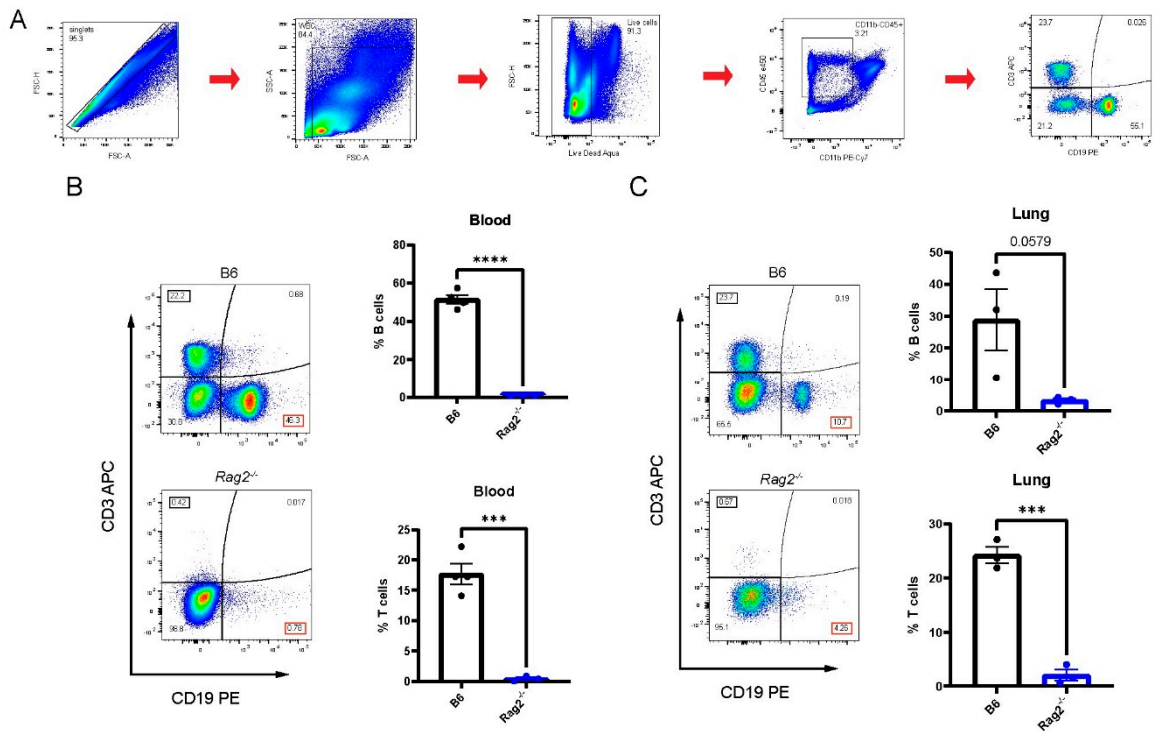
Supplemental Figure S2. Viral infection in AT2 cells was identified by co-staining surfactant protein C (Spc) with SARS-CoV2 spike (S) protein. Representative images from 20-week-old *K18-hACE2* (top) and B6 mice (bottom), which were intranasally infected with CoV2 MA30 (5×10^4 TCID₅₀) and CoV2 MA1 (1×10^4 TCID₅₀), respectively, and sacrificed at 3 DPI. SARS S protein in green, Spc in magenta, DAPI in white and merged channels with red arrows signaling co-localization of Spc and SARS S protein.



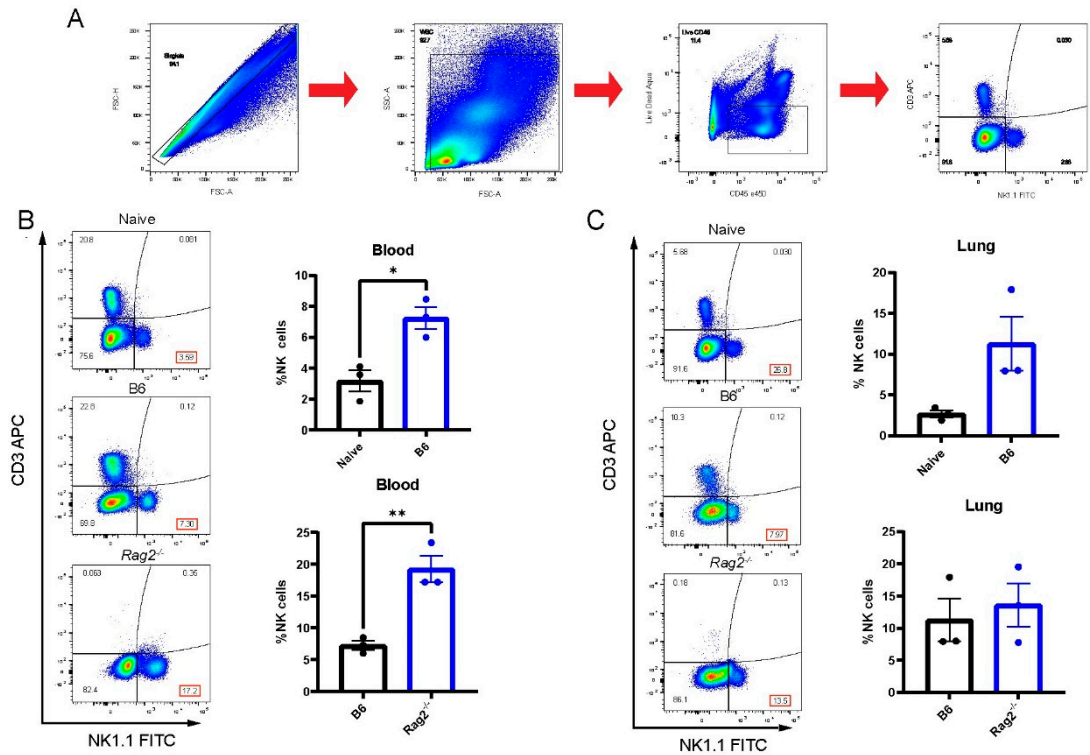
Supplemental Figure S3. Increased SARS-CoV2 Spike protein staining in lungs of the infected *Rag2^{-/-}* mice. (A, B) Images of pulmonary sections for immunofluorescence staining of five different *Rag2^{-/-}* mice (A) and five different B6 mice (B) infected with MA30 (5×10^4 TCID₅₀ IN) at 15 DPI. Anti-SARS S protein antibody in green and DAPI in white.



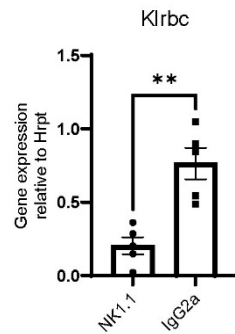
Supplemental Figure S4. No difference in inflammation in MA30-infected *Rag2*^{-/-} and B6 mice at 15 days post infection (DPI). (A, B) Representative images of H/E stains for areas of inflammation in the infected B6 and *Rag2*^{-/-} male lungs at 15 DPI (MA30, 5 X 10⁴, TCID₅₀, IN). (C) Quantification of B6 and *Rag2*^{-/-} male mice showed no significant difference.



Supplemental Figure S5. Flow cytometry analysis of T and B cells from the PBMC and lung cells of B6 and *Rag2*^{-/-} mice at 3 DPI (MA30, 1 X 10⁴, TCID₅₀, IN). (A) Gating strategy showing sequence and filtration of cells from left to right. (BC) Representative images showing percent T (black box, quadrant 1) and B cells (red box, quadrant 3) in PBMC (B) and lungs (C) of infected mice. Quantification of all mice with significant statistics shown by asterisks (***p* < 0.001; and *****p* < 0.0001) using unpaired *t*-test.



Supplemental Figure S6. Flow cytometry analysis of NK cells from the PBMC and lung cells of naive, B6 and *Rag2*^{-/-} mice at 3 DPI (MA30, 1 X 10⁴, TCID₅₀, IN). (A) Gating strategy showing sequence and filtration of cells from left to right. (BC) Representative images showing percent NK cells (red box, quadrant 3) in PBMC (B) and lungs (C) of naive vsinfected mice, and infected mice vs. infected *Rag2*^{-/-} mice. Quantification of all mice with significant statistics shown by asterisks (* $p < 0.05$ and ** $p < 0.01$) using unpaired *t*-test.



Supplemental Figure S7. Treatment of *Rag2*^{-/-} mice with NK1.1 depletes NK cells. (A) Male *Rag2*^{-/-} mice depleted with anti-NK1.1 compared to isotype control IgG2a treated-mice showed significant difference (** $p < 0.001$ using unpaired *t*-test) in the lungs for Klrbc expression levels, a gene marker for NK cell presence, normalized to Hrpt, a housekeeping gene.